The Journal of Chemical Physics

To see C_2: Single-photon ionization of the dicarbon molecule

Cite as: J. Chem. Phys. **152**, 041105 (2020); https://doi.org/10.1063/1.5139309
Submitted: 20 November 2019 . Accepted: 10 January 2020 . Published Online: 29 January 2020

Oliver J. Harper, Séverine Boyé-Péronne, Gustavo A. Garcia, Helgi R. Hrodmarsson, Jean-Christophe Loison, and Bérenger Gans

AIP Publishing

The Journal of Chemical Physics | COMMUNICATION | scitation.org/journal/jcp

To see C_2: Single-photon ionization of the dicarbon molecule

Cite as: J. Chem. Phys. 152, 041105 (2020); doi: 10.1063/1.5139309
Submitted: 20 November 2019 • Accepted: 10 January 2020 •
Published Online: 29 January 2020

Oliver J. Harper,[1] Séverine Boyé-Péronne,[1] Gustavo A. Garcia,[2] Helgi R. Hrodmarsson,[2,a)] Jean-Christophe Loison,[3] and Bérenger Gans[1,b)]

AFFILIATIONS

[1]Institut des Sciences Moléculaires d'Orsay, CNRS, Université Paris-Saclay, 91405 Orsay, France
[2]Synchrotron SOLEIL, L'Orme des Merisiers, Saint Aubin BP 48, F-91192 Gif sur Yvette Cedex, France
[3]Institut des Sciences Moléculaires, UMR 5255 CNRS–Université de Bordeaux, Bât. A12, 351 cours de la Libération, F-33405 Talence Cedex, France

[a)]**Present address:** Sackler Laboratory for Astrophysics, Leiden Observatory, Leiden University, Leiden, The Netherlands.
[b)]**Author to whom correspondence should be addressed:** berenger.gans@u-psud.fr

ABSTRACT

The C_2 carbon cluster is found in a large variety of environments including flames, electric discharges, and astrophysical media. Due to spin-selection rules, assessing a complete overview of the dense vibronic landscape of the C_2^+ cation starting from the ground electronic state $X\ ^1\Sigma_g^+$ of the neutral is not possible, especially since the C_2^+ ground state is of $X^+\ ^4\Sigma_g^-$ symmetry. In this work, a flow-tube reactor source is employed to generate the neutral C_2 in a mixture of both the lowest singlet $X\ ^1\Sigma_g^+$ and triplet $a\ ^3\Pi_u$ electronic states. We have investigated the vibronic transitions in the vicinity of the first adiabatic ionization potential via one-photon ionization with vacuum ultraviolet synchrotron radiation coupled with electron/ion double imaging techniques. Using *ab initio* calculations and Franck-Condon simulations, three electronic transitions are identified and their adiabatic ionization energy is determined $E_i(a^+\ ^2\Pi_u \leftarrow X\ ^1\Sigma_g^+) = 12.440(10)$ eV, $E_i(X^+\ ^4\Sigma_g^- \leftarrow a\ ^3\Pi_u) = 11.795(10)$ eV, and $E_i(a^{+2}\Pi_u \leftarrow a^3\Pi_u) = 12.361(10)$ eV. From the three origin bands, the following energy differences are extracted: $\Delta E(a - X) = 0.079(10)$ eV and $\Delta E(a^+ - X^+) = 0.567(10)$ eV. The adiabatic ionization potential corresponding to the forbidden one-photon transition $X^+ \leftarrow X$ is derived and amounts to 11.873(10) eV, in very good agreement with the most recent measurement by Krechkivska *et al.* [J. Chem. Phys. **144**, 144305 (2016)]. The enthalpy of formation of the doublet ground state C_2^+ cation in the gas phase is determined at 0 K, $\Delta_f H^0(0K)(C_2^+(^2\Pi_u)) = 2019.9(10)$ kJ mol^{-1}. In addition, we report the first experimental ion yield of C_2 for which only a simple estimate was used up to now in the photochemistry models of astrophysical media due to the lack of experimental data.

The dicarbon molecule (C_2) is ubiquitous in many environments such as flames,[1,2] plasmas, and astrophysical media,[3,4] being the first transient species to have been identified in the coma of a comet.[5] The omnipresence of C_2 in diffuse interstellar clouds allowed some Diffuse Interstellar Bands to be named C_2-DIBs because they are detected in interstellar clouds that are characterized by high column densities of C_2 molecules.[6] Given the intense UV radiation in these environments, the quantification of C_2 photoionization is important as this constitutes a source of C_2^+, which is a much more reactive species than C_2 which only reacts slowly with H_2.[7,8] Although the absorption and emission spectroscopies of this species and its cation have been extensively studied theoretically and experimentally, photoionization studies were mainly limited to theoretical works.[9–11] Only recently, Krechkivska *et al.* reported for the first time a measurement of its adiabatic ionization potential (IP) ($X^+\ ^4\Sigma_g^- \leftarrow X\ ^1\Sigma_g^+$) using resonant two-photon threshold-ionization spectroscopy.[12] In their work, they produced C_2 in its $a\ ^3\Pi_u$ metastable state using an electric discharge and ionized it toward its cationic ground state through the neutral $4\ ^3\Pi_g$ electronic state. To our knowledge, no single-photon ionization experiment has been performed up to now. The ground electronic states of C_2 and C_2^+ being $X\ ^1\Sigma_g^+$ and $X^+\ ^4\Sigma_g^-$, a single-photon

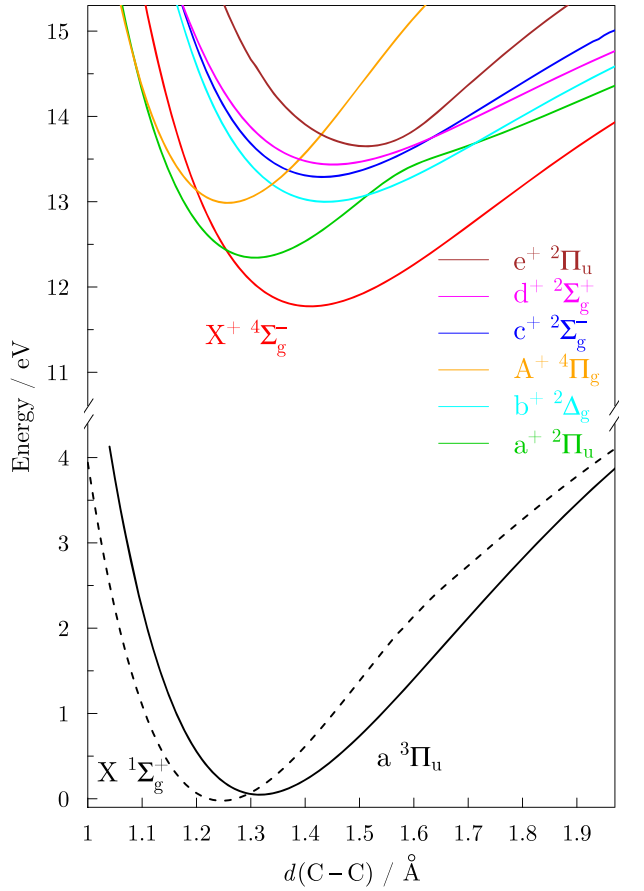

FIG. 1. Calculated potential energy surfaces of C_2 and C_2^+ as a function of the d(C–C) distance.

ionizing transition between these two states is spin-forbidden. Thus, C_2 must be photoionized from the $a^3\Pi_u$ metastable state to reach the cation ground state. In order to have a complete overview of the photoionization of C_2, it is necessary to use broadly tunable vacuum ultraviolet (VUV) radiation coupled to a sensitive mass-selective photoelectron spectrometer, C_2 being generally produced in a complex mixture containing several species and in small quantities.

In this paper, we report the first single-photon ionization of C_2 in the vicinity of the adiabatic ionization potential (IP). The experiments were performed at the DESIRS beamline[13] of the French SOLEIL synchrotron facility. All of the experimental details have been described previously.[14,15] F atoms, produced by a microwave discharge applied to F_2, and CH_4 diluted in He were introduced in the flow-tube reactor. The experimental conditions (gas flow and relative concentrations) were optimized in order to produce C_2 by secondary reactions. In these conditions, several species were generated (CH_x, C_2H_x, C_3H_x, ... with x = 0, 1, 2, ...). Due to the exothermicity of consecutive H abstractions and secondary reactions, the products can be formed with high vibrational temperature and in excited metastable states. The resulting gas flow is then skimmed twice before crossing at right angle the monochromatized synchrotron radiation in the double-imaging photoelectron/photoion spectrometer DELICIOUS III. The photon resolution in the range of 11.5–14 eV was δE = 9 meV. The spectrum was corrected for photon flux fluctuations using the photodiode (AXUV100, IRD) current recorded over the scan range. The photoelectrons were extracted by an 88 V/cm field, and the offline analysis of their corresponding mass-selected velocity map images was set to provide a total resolution, including the photon energy contribution, of approximately 25 meV on the threshold photoelectron (TPE) spectrum, which was obtained applying the slow photoelectron (SPE) method described previously.[16] The absolute calibration of the energy scale was performed using argon lines (present in the gas filter of the

TABLE I. C_2 and C_2^+ electronic state energies extrapolated to the CBS limit (see text).

Species	State	Main configurations[a]	E (CBS) (hartree)	$E_{I,calc.}$[b] (eV)
C_2	$X\,^1\Sigma_g^+$	$71\%\ (2\sigma_u)^2(1\pi_u)^4 + 14\%(2\sigma_u)^0(1\pi_u)^4(3\sigma_g)^2$	−75.811 535	0.000
	$a\,^3\Pi_u$	$88\%\ (2\sigma_u)^2(1\pi_u)^3(3\sigma_g)^1 + 5\%(2\sigma_u)^1(1\pi_u)^2(3\sigma_g)^2(1\pi_g)^1$	−75.809 599	0.053
C_2^+	$X^+\,^4\Sigma_g^-$	$86\%\ (2\sigma_u)^2(1\pi_u)^2(3\sigma_g)^1 + 7\%(2\sigma_u)^1(1\pi_u)^1(3\sigma_g)^2(1\pi_g)^1$	−75.377 781	11.803
	$a^+\,^2\Pi_u$	$72\%(2\sigma_u)^2(1\pi_u)^3 + 13\%(2\sigma_u)^0(1\pi_u)^3(3\sigma_g)^2$	−75.356 565	12.381
	$A^+\,^4\Pi_g$	$86\%(2\sigma_u)^1(1\pi_u)^3(3\sigma_g)^1 + 6\%(2\sigma_u)^2(1\pi_u)^2(1\pi_g)^1$	−75.333 358	13.012
	$b^+\,^2\Delta_g$	$88\%\ (2\sigma_u)^2(1\pi_u)^2(3\sigma_g)^1$	−75.332 633	13.032
	$c^+\,^2\Sigma_g^-$	$88\%\ (2\sigma_u)^2(1\pi_u)^2(3\sigma_g)^1$	−75.322 311	13.313
	$d^+\,^2\Sigma_g^+$	$82\%\ (2\sigma_u)^2(1\pi_u)^2(3\sigma_g)^1$	−75.316 892	13.460
	$e^+\,^2\Pi_u$	$85\%\ (2\sigma_u)^2(1\pi_u)^1(3\sigma_g)^2$	−75.308 704	13.683[c]

[a]Main contributing configurations calculated at the optimized geometry of each state. For the sake of clarity, the common part of the configuration, i.e., $(1\sigma_g)^2(1\sigma_g)^2(2\sigma_g)^2$, is omitted, and the configurations contributing to less than 5% are disregarded.
[b]Calculated ionization energy with respect to the $X\,^1\Sigma_g^+$ neutral ground state.
[c]Regarding the main configurations, the photoionizing transitions toward the e^+ state can only occur thanks to configuration mixing and are thus expected to be very weak.

beamline) seen as dips in the ionization signal during the energy scan leading to an error on the absolute energy scale of 7 meV. A Gaussian multi-peak least-squares fit was performed to locate the band positions. The fit pointing errors were deduced as described in Ref. 17 and convoluted with the energy scale precision. E_I values were also corrected by the field-induced shift (−7 meV) resulting from the 88 V/cm extraction field used in the spectrometer. The overall accuracy of the ionization energies (E_I) is estimated at 10 meV (2σ uncertainty).

The *ab initio* calculations on the electronic states of C_2 and C_2^+ were carried out using the internally contracted multireference configuration interaction method with Davidson correction (MRCI+Q) with complete active space self-consistent field (CASSCF) wavefunctions. The CASSCF and MRCI calculations were performed at full valence, namely, with 12 (11 for C_2^+) electrons distributed in 12 orbitals with the 1s orbitals of carbon atoms kept doubly occupied but fully optimized. All calculations were performed using the MOLPRO 2012 package.[18] The potential energy curves of the two lowest electronic states of C_2 and the seven lowest electronic states of C_2^+ were computed as a function of C–C bond length d(C–C). Harmonic vibrational wavenumbers were calculated through the standard MOLPRO procedure using the Hessian and normal modes. Complete basis set (CBS) extrapolations were carried out using the VnZ (n = T, Q, 5, and 6) basis set series. The CASSCF and dynamical correlation ($E_{MRCI+Q} - E_{CASSCF}$) energies were extrapolated using the $E_{CASSCF}(CBS) + A \times \exp(-B \times n)$ and $E_{Corr}(CBS) + C \times n^{-3}$ functions, respectively. The calculated energies given in this paper correspond to $E(CBS) = E_{CASSCF}(CBS) + E_{Corr}(CBS)$. Franck–Condon (FC) spectrum simulations were carried out by means of the PGOPHER software, using our *ab initio* results as input data.[19]

As reported by several theoretical works,[9,20,21] the energetic landscape of C_2^+ from its ground state up to only 3 eV is very dense. In Fig. 1, our calculated potential energy surfaces are displayed vs the d(C–C) bond distance for the two lowest electronic states of C_2 and the seven lowest electronic states of C_2^+. The energies calculated at the equilibrium geometries obtained in the VnZ basis sets (n = T, Q, 5, and 6) were extrapolated as a function of the n cardinal number to estimate the CBS limit for each state. The resulting energies with respect to the C_2 ground state energy are reported in Table I.

From Fig. 1 and the main configurations of Table I, only one direct photoionizing transition from the $X\,^1\Sigma_g^+$ electronic ground state should be allowed below 14 eV, namely, $a^+\,^2\Pi_u \leftarrow X\,^1\Sigma_g^+$, and six are possible from the $a\,^3\Pi_u$ metastable state. However, according to Ref. 11, two more photoionizing transitions involving the states of $^2\Sigma_g$ symmetry are also expected from the $X\,^1\Sigma_g^+$ state through shake-up processes, i.e., $c^+\,^2\Sigma_g^- \leftarrow X\,^1\Sigma_g^+$ and $d^+\,^2\Sigma_g^+ \leftarrow X\,^1\Sigma_g^+$. Using the *ab initio* output files of our calculations, we have performed a Franck–Condon (FC) simulation of each transition with the PGOPHER software neglecting spin.[19] For that purpose, we directly used the MOLDEN output files calculated with AVQZ basis for all states except the d^+ state (with AVTZ basis) because of convergence issues. The adiabatic energy levels obtained by the CBS extrapolations were also implemented in PGOPHER.

These simulations are compared with the experimental TPE spectrum of C_2 in Fig. 2. From this figure, one can readily assign three different photoionizing transitions between 11.4 eV and 12.7 eV:

- $X^+\,^4\Sigma_g^-(v^+) \leftarrow a\,^3\Pi_u(v)$,
- $a^+\,^2\Pi_u(v^+ = 0) \leftarrow a\,^3\Pi_u(v = 0)$, and
- $a^+\,^2\Pi_u(v^+) \leftarrow X\,^1\Sigma_g^+(v)$.

Above 12.7 eV, the assignment is more complicated due to the numerous vibronic transitions, their weak oscillator strengths, and the low signal-to-noise ratio of the experimental signal. It is, nevertheless, clear that other transitions occur especially around 13 eV, 13.2 eV, and 13.6 eV where net signals are observed.

Using the FC simulations of the three assigned transitions and fitting the adiabatic ionization potentials (IPs) and the vibronic band

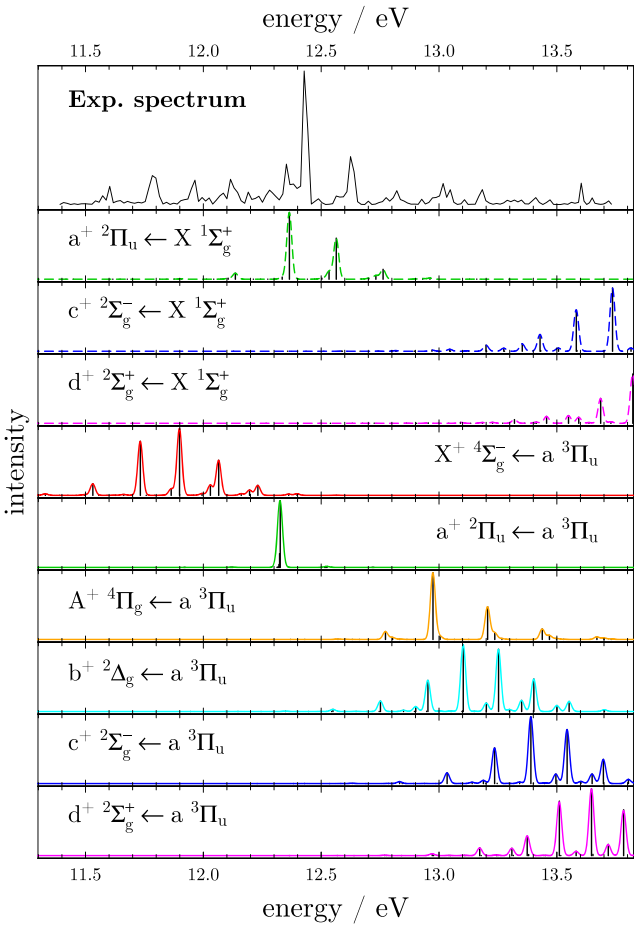

FIG. 2. Experimental photoelectron spectrum of C_2 (upper panel) compared with the calculated spectra (using our FC simulation and our calculated adiabatic energies) of each vibronic photoionizing transition predicted in the measurement energy range (nine lower panels). Note that the same color code as the one in Fig. 1 for the upper state is used. Full-line calculated spectra correspond to photoionization from the a $^3\Pi_u$ state, whereas dashed line spectra correspond to photoionization from the $X\,^1\Sigma_g^+$ ground state. For the nine lowest panels, the black stick spectra correspond to the FCF simulation and the full or dashed colored lines to the corresponding convolutions with a Gaussian-line shape (FWHM = 25 meV).

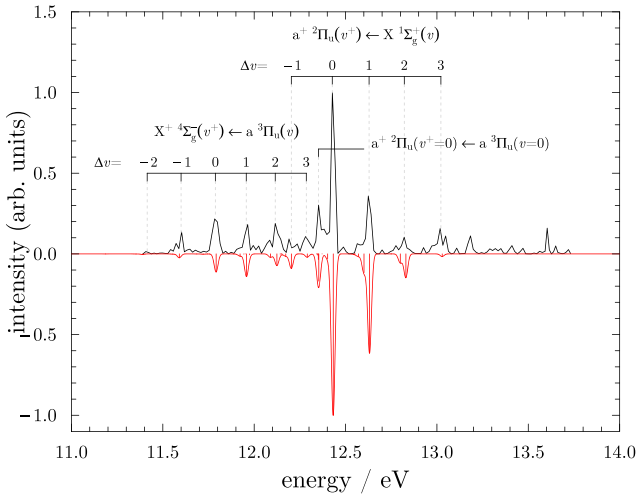

FIG. 3. Experimental photoelectron spectrum of C_2 (upper panel) compared with our simulated spectrum (obtained by summing of the FC simulations of the $X^+\,^4\Sigma_g^- \leftarrow a\,^3\Pi_u$, $a^+\,^2\Pi_u \leftarrow X\,^1\Sigma_g^+$, and $a^+\,^2\Pi_u \leftarrow a\,^3\Pi_u$ photoionizing transitions and using our fitted ionization energies) (lower panel). The red stick spectrum corresponds to the FC simulation and the red curve to its convolution with a Gaussian-line-shape (FWHM = 25 meV).

intensities on the experimental data, we performed the simulation of the experimental spectrum depicted in Fig. 3. The vibrational temperature used in the simulation was set to 1500 K, and the vibronic band intensities were manually adjusted to 1.00, 0.60, and 0.42 for the $a^+\,^2\Pi_u \leftarrow X\,^1\Sigma_g^+$, $X^+\,^4\Sigma_g^- \leftarrow a\,^3\Pi_u$, and $a^{+2}\Pi_u \leftarrow a^3\Pi_u$ transitions, respectively. The agreement is very satisfactory, strengthening our assignment.

From the experimental positions of the origin bands, we can then extract the adiabatic IP for the three allowed-photoionizing transitions. These values corrected by the field-induced Stark shift (−7 meV) are reported in Table II. The adiabatic IP obtained for the $X^+\,^4\Sigma_g^- \leftarrow a\,^3\Pi_u$ transition is in very good agreement with that of Krechkivska *et al.* [11.791(5) eV].[12] In the case of the $a^+\,^2\Pi_u \leftarrow X\,^1\Sigma_g^+$ and $a^{+2}\Pi_u \leftarrow a^3\Pi_u$ transitions, no other measurement has been reported in the literature but for this work. Combining the three origin bands, we derive the singlet-triplet and quadruplet-doublet energy differences in the neutral and cationic species, respectively, $\Delta E(a - X) = 0.079(10)$ eV and $\Delta E(a^+ - X^+) = 0.567(10)$ eV. Our $\Delta E(a - X)$ value is in very good agreement with the zero-point energy derived from the rotationally resolved analysis of Chen *et al.* [613.650(3) cm^{-1} = 76 meV].[22] To our knowledge, there is no other measurement of $\Delta E(a^+ - X^+)$ in the literature. In addition, we extract the adiabatic IP of the forbidden $X^+\,^4\Sigma_g^- \leftarrow X\,^1\Sigma_g^+$ photoionizing transition $E_i(X^+ \leftarrow X) = 11.873(10)$ eV, in very good agreement with the one derived in 2016 by Krechkivska *et al.* [11.866(5) eV].[12] Using the gas-phase enthalpy of formation of the quadruplet ground state of the C_2^+ cation at 0 K from the active thermochemical tables [23–25] [i.e., $\Delta_f H^0(0K)(C_2^+(^4\Sigma_g^+)) = 1965.2$ kJ mol^{-1}] and our measured $\Delta E(a^+ - X^+) = 54.7(10)$ kJ mol^{-1}, we determine the enthalpy of formation of the lowest doublet state of the C_2^+ cation, $\Delta_f H^0(0K)(C_2^+(^2\Pi_u)) = 2019.9(10)$ kJ mol^{-1}. From the vibrational structures of the $X^+\,^4\Sigma_g^- \leftarrow a\,^3\Pi_u$ and $a^+\,^2\Pi_u \leftarrow X\,^1\Sigma_g^+$ transitions, we also extract the vibrational fundamentals of the $X^+\,^4\Sigma_g^-$ and $a^+\,^2\Pi_u$ electronic states of C_2^+, $\nu_0(X^+) = 1460(80)$ cm^{-1} and $\nu_0(a^+) = 1590(80)$ cm^{-1}, respectively.

In addition to these results, the C_2 ionization yield has been measured and is reported in Fig. 4. Despite the low signal-to-noise ratio, several reproducible structures are observed at 11.814 eV,

TABLE II. Adiabatic ionization energies of C_2.

	$E_{I,calc.}$ (eV)		$E_{I,calc.corr.ZPE}$ (eV)	$E_{I,expt.}$ (eV)	
Transition	Reference 10[a]	This work[b]	This work[b]	Reference 12[c]	This work[d]
$X^+\,^4\Sigma_g^- \leftarrow X\,^1\Sigma_g^+$[e]	...	11.803	11.771	11.866(5)	11.873(10)
$a^+\,^2\Pi_u \leftarrow X\,^1\Sigma_g^+$	12.40	12.381	12.365	...	12.440(10)
$c^+\,^2\Sigma_g^- \leftarrow X\,^1\Sigma_g^+$	...	13.313	13.275	...	...
$d^+\,^2\Sigma_g^+ \leftarrow X\,^1\Sigma_g^+$	...	13.460	13.413	...	...
$X^+\,^4\Sigma_g^- \leftarrow a\,^3\Pi_u$	11.75	11.750	11.733	11.791(5)	11.795(10)
$a^+\,^2\Pi_u \leftarrow a\,^3\Pi_u$	12.29	12.328	12.326	...	12.361(10)
$A^+\,^4\Pi_g \leftarrow a\,^3\Pi_u$	...	12.959	12.974	...	...
$b^+\,^2\Delta_g \leftarrow a\,^3\Pi_u$	...	12.979	12.953	...	...
$c^+\,^2\Sigma_g^- \leftarrow a\,^3\Pi_u$	...	13.260	13.236	...	...
$d^+\,^2\Sigma_g^+ \leftarrow a\,^3\Pi_u$	...	13.404	13.374	...	...

[a]CCSD(T) values.
[b]Derived from the complete basis set (CBS) limit extrapolations and corrected by the zero point energies (ZPE) of the neutral and cationic states when indicated.
[c]Resonant two-photon threshold ionization spectroscopy.
[d]Fitted values used in Fig. 3 corrected by the field-induced shift.
[e]Forbidden transition.

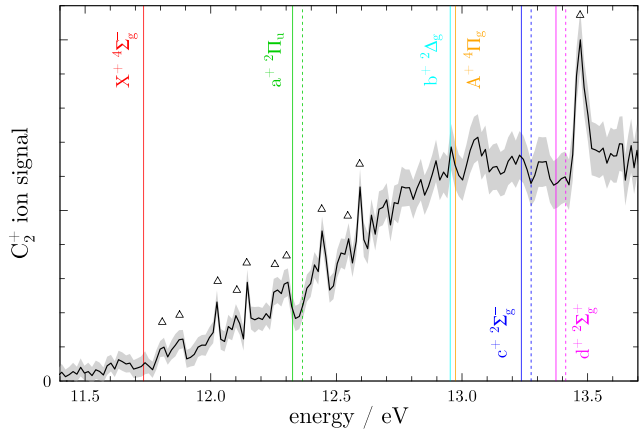

FIG. 4. C_2^+ ion yield (black full line) as a function of the photon energy and its statistical error (gray shaded area). The structures marked by open triangles are caused by autoinizing Rydberg states. The transition energies ($E_{I,calc.corr.ZPE}$) of Table II are reported as dashed and full vertical lines for transitions from the singlet and from the triplet electronic states of the neutral, respectively. The color code is identical to Figs. 1 and 2.

11.889 eV, 12.025 eV, 12.100 eV, 12.145 eV, 12.266 eV, 12.307 eV, 12.443 eV, 12.549 eV, 12.594 eV, and 13.47 eV. We attribute these features to autoionization processes. However, the assignment of the involved Rydberg states is not straightforward. Indeed, in the experiment, both the lowest singlet and triplet states of C_2 are populated and many electronic states of the cation lie within the explored energy range. Hence, several Rydberg series are superimposed in the spectrum. The autoionization structures have been discussed by Toffoli and Lucchese,[11] but only above 13 eV. The comparison with our experiment is thus not possible. Nevertheless, below 13 eV, the sharpest structures might be the signature of Rydberg series converging toward excited states of the cation above the a^+ state. These Rydberg series are most probably reached from the triplet metastable state of the neutral, and they autoionize into the X^+ or the a^+ cationic states. Note that electronic and vibrational autoionization processes might coexist in this energy range for C_2 like in the case of the CH radical.[15] Higher resolved ion yield spectra of C_2 in its ground state only and in its two lowest electronic states are necessary to study in detail the autoionization processes of this system. In astrophysical models, the photoionization cross section of C_2 is assumed to be zero below the estimated IP (12.16 eV) and constant above this energy.[26] Although the assignment of this ion yield still has to be performed, the data clearly show that the crude estimated ion yield used in the astrophysical models should be revised.

To conclude, the new results presented in this paper significantly improve the spectroscopic knowledge of the dicarbon cation. They should stimulate future high-resolution experiments employing the present radical source to further refine the values of the ionization energies, to help in identifying the autoionization structures, and to disentangle the vibronic transitions observed above 13 eV.

This work was performed on the DESIRS beamline under Proposal No. 20181543. The authors acknowledge SOLEIL for provision of synchrotron radiation facilities and the DESIRS beamline team for their assistance. This work was supported by the French Agence Nationale de la Recherche (ANR) under Grant No. ANR-12-BS08-0020-02 (Project SYNCHROKIN) and by the Programme National "Physique et Chimie du Milieu Interstellaire" (PCMI) of CNRS/INSU with INC/INP co-funded by CEA and CNES.

REFERENCES

[1] W. H. Wollaston, "XII. A method of examining refractive and dispersive powers, by prismatic reflection," Philos. Trans. R. Soc. London **92**, 365–380 (1802).
[2] A. G. Gaydon, in The Spectroscopy of Flames, 2nd ed., edited by TAC Ltd. (Springer, Dordrecht, Edinburgh, 1974).
[3] R. C. Hupe, Y. Sheffer, and S. R. Federman, "Ultraviolet measurements of interstellar C_2," Astrophys. J. **761**, 38 (2012).
[4] S. Hamano, H. Kawakita, N. Kobayashi, K. Takenaka, Y. Ikeda, N. Matsunaga, S. Kondo, H. Sameshima, K. Fukue, C. Yasui, M. Mizumoto, S. Otsubo, A. Watase, T. Yoshikawa, and H. Kobayashi, "First detection of A–X (0,0) bands of interstellar C_2 and CN," Astrophys. J. **881**, 143 (2019).
[5] G. Donati, "Schreiben des Herrn Professors Donati an den Herausgeber," Astron. Nachr. **62**, 376 (1864).
[6] M. Elyajouri, R. Lallement, N. L. J. Cox, J. Cami, M. A. Cordiner, J. V. Smoker, A. Fahrang, P. J. Sarre, and H. Linnartz, "The EDIBLES survey. III. C_2-DIBs and their profiles," Astron. Astrophys. **616**, A143 (2018).
[7] V. G. Anicich, "An index of the literature for bimolecular gas phase cation-molecule reaction kinetics," JPL-Publication-03-19, 2003.
[8] M. Nakajima, A. Matsugi, and A. Miyoshi, "Mechanism and kinetic isotope effect of the reaction of $C_2(X^1\Sigma_g^+)$ radicals with H_2 and D_2," J. Phys. Chem. A **113**, 8963–8970 (2009).
[9] G. Verhaegen, "Theoretical calculation of the electronic states of C_2^+," J. Chem. Phys. **49**, 4696–4705 (1968).
[10] J. D. Watts and R. J. Bartlett, "Coupled-cluster calculations on the C_2 molecule and the C_2^+ and C_2^- molecular ions," J. Chem. Phys. **96**, 6073–6084 (1992).
[11] D. Toffoli and R. R. Lucchese, "Near threshold photoionization of the ground and first excited states of C_2," J. Chem. Phys. **120**, 6010–6018 (2004).
[12] O. Krechkivska, G. B. Bacskay, B. A. Welsh, K. Nauta, S. H. Kable, J. F. Stanton, and T. W. Schmidt, "The ionization energy of C_2," J. Chem. Phys. **144**, 144305 (2016).
[13] L. Nahon, N. de Oliveira, G. A. Garcia, J.-F. Gil, B. Pilette, O. Marcouillé, B. Lagarde, and F. Polack, "DESIRS: A state-of-the-art VUV beamline featuring high resolution and variable polarization for spectroscopy and dichroism at SOLEIL," J. Synchrotron Radiat. **19**, 508–520 (2012).
[14] G. A. Garcia, X. Tang, J.-F. Gil, L. Nahon, M. Ward, S. Batut, C. Fittschen, C. A. Taatjes, D. L. Osborn, and J.-C. Loison, "Synchrotron-based double imaging photoelectron/photoion coincidence spectroscopy of radicals produced in a flow tube: OH and OD," J. Chem. Phys. **142**, 164201 (2015).
[15] B. Gans, F. Holzmeier, J. Krüger, C. Falvo, A. Röder, A. Lopes, G. A. Garcia, C. Fittschen, J.-C. Loison, and C. Alcaraz, "Synchrotron-based valence shell photoionization of CH radical," J. Chem. Phys. **144**, 204307 (2016).
[16] J. C. Poully, J. P. Schermann, N. Nieuwjaer, F. Lecomte, G. Gregoire, C. Desfrancois, G. A. Garcia, L. Nahon, D. Nandi, L. Poisson, and M. Hochlaf, "Photoionization of 2-pyridone and 2-hydroxypyridine," Phys. Chem. Chem. Phys. **12**, 3566–3572 (2010).
[17] J. W. Brault, "High precision fourier transform spectrometry: The critical role of phase corrections," Microchim. Acta **93**, 215–227 (1987).
[18] H. J. Werner, P. J. Knowles, G. Knizia, F. R. Manby, M. Schütz *et al.*, MOLPRO, version 2012.1, a package of *ab initio* programs, 2012.
[19] C. M. Western, "PGOPHER: A program for simulating rotational, vibrational and electronic spectra," J. Quant. Spectrosc. Radiat. Transfer **186**, 221–242 (2017).
[20] C. Petrongolo, P. J. Bruna, S. D. Peyerimhoff, and R. J. Buenker, "Theoretical prediction of the potential curves for the lowest-lying states of the C_2^+ molecular ion," J. Chem. Phys. **74**, 4594–4602 (1981).

[21] P. Rosmus, H.-J. Werner, E.-A. Reinsch, and M. Larsson, "Multireference CI calculations of radiative transition probabilities between low lying quartet states of the C_2^+ ion," J. Electron Spectrosc. Relat. Phenom. **41**, 289–296 (1986).
[22] W. Chen, K. Kawaguchi, P. F. Bernath, and J. Tang, "Simultaneous analysis of the Ballik-Ramsay and Phillips systems of C_2 and observation of forbidden transitions between singlet and triplet states," J. Chem. Phys. **142**, 064317 (2015).
[23] B. Ruscic, R. E. Pinzon, M. L. Morton, G. von Laszevski, S. J. Bittner, S. G. Nijsure, K. A. Amin, M. Minkoff, and A. F. Wagner, "Introduction to active thermochemical tables:several "key" enthalpies of formation revisited," J. Phys. Chem. A **108**, 9979–9997 (2004).
[24] B. Ruscic, R. E. Pinzon, G. von Laszewski, D. Kodeboyina, A. Burcat, D. Leahy, D. Montoy, and A. F. Wagner, "Active thermochemical Tables: Thermochemistry for the 21st century," J. Phys.: Conf. Ser. **16**, 561–570 (2005).
[25] B. Ruscic and D. H. Bross, "Active thermochemical tables (ATcT) values based on ver. 1.122 g of the thermochemical network," Argonne National Laboratory, 2019, available at ATcT.anl.gov, 2019.
[26] A. N. Heays, A. D. Bosman, and E. F. van Dishoeck, "Photodissociation and photoionisation of atoms and molecules of astrophysical interest," Astron. Astrophys. **602**, A105 (2017).